

Immuno-regulated common markers but different network signatures in two associated cancers: evidences from epigenetic treatment

Enrico Capobianco^{1,2}

¹Center for Computational Science, Miller School of Medicine, University of Miami, Miami, FL 33146, USA; ²Laboratory of Integrative Systems Medicine, Institute of Clinical Physiology, National Research Council, Pisa, Italy

Correspondence to: Enrico Capobianco. Center for Computational Science, Miller School of Medicine, University of Miami, Miami, FL 33146, USA. Email: ecapobianco@med.miami.edu.

Background: Networks are now widely accepted inference tools in translational oncology. Besides providing agnostic model frameworks for complex data-driven clinical problems of diagnostic, therapeutic and prognostic impacts, networks mainly support insights, testable hypotheses and decision processes on the basis of their topological configurations and connectivity patterns.

Methods: The purpose of this study is to emphasize the role of both gene and network signatures in two specific cancers. Retinoblastoma (RB) and osteosarcoma are associated to some extent. It is known that patients who carry germline mutations in the *RBI* gene, and who survive RB, are typically at an increased risk of early-onset second cancers, including osteosarcomas. Gene signatures are widely used, but also criticized for their partial lack of reproducibility. Network signatures include gene association dynamics by identifying modules or communities in which subsets of genes functionally belong.

Results: Two cancer cell lines (one per cancer type) were subjected to a similar epigenetic treatment regimen, using a demethylation agent (DAC, and including similar dose and time course administration). A minimal set of shared differentially expressed (DEG) genes was identified in cancer-specific cell lines from microarray analyses. However, the identified immune signatures were observed to translate into much diversified network signatures.

Conclusions: Our evidence is relevant to therapeutic developments, indicating that preference should be assigned to the assessment of bio-entities in a connected environment rather than considering single entities alone.

Keywords: Cancer; molecular therapeutics; epigenetics; translational network medicine

Submitted Jan 25, 2016. Accepted for publication Feb 01, 2016.

doi: [10.21037/atm.2016.02.14](https://doi.org/10.21037/atm.2016.02.14)

View this article at: <http://dx.doi.org/10.21037/atm.2016.02.14>

Introduction

The retinoblastoma (RB) susceptibility gene *RBI* is known to play a causal role in human cancer (1-3). In particular, the gene inactivation in chromosome band 13q14 has revealed RB formation, an identification which was derived from specific mutations. The *RBI* gene and its protein explain key mechanisms of oncogenesis, development, and gene regulation, and help our understanding of genetic diagnosis of susceptibility for other *RBI*-dysfunction driven cancers, such as the human osteosarcoma (HOS) (4). In the past, a few hereditary HOS risk factors have been identified, but

these rare events account for relatively few patients. It is also well-known, however, that survivors of the inherited form of RB are at an increased risk to develop second primary HOS compared to the general population or to survivors of non-inherited RB (5).

Cancer is considered to be a genetic disease, but other types of alterations are exerting influences. For instance, epigenetic modifications may regulate gene expression and, thus, cancer development. Epigenetic dysregulation may precede other transforming events, ranging from focal mutations to genome-wide instability (6,7). Especially recent

Table 1 Relevant RB DEGs

| GO term | P value | Genes | FDR |
|--|----------|--|----------|
| Regulation of cell death | 4.31E-19 | <i>MNT, TUBB, BBC3, MADD, BOK, CDKN2A, TAX1BP1, TICAM1, PEA15, MALT1, DAP, HSPA1A, IRAK1, CDKN1A, IKBKG, TIAF1, MKL1, TRAF2, BAK1, TP53, BCL2L1, BAX, BIK, TRADD, RELA*, FAS, DAXX, TP73*, MAPK8IP1</i> | 5.84E-16 |
| Programmed cell death | 5.37E-13 | <i>TIAF1, BBC3, PIDD, BOK, MADD, CDKN2A, TICAM1, TAX1BP1, PEA15, TRAF2, BAK1, TP53, TNFRSF1A, DAP, BCL2L1, BAX, BIK, TRADD, FAS, TP73*, DAXX</i> | 7.28E-10 |
| Positive regulation of cell death | 2.67E-12 | <i>TUBB, BBC3, BOK, CDKN2A, TICAM1, TRAF2, BAK1, TP53, DAP, BCL2L1, BAX, BIK, TRADD, FAS, CDKN1A, TP73*, DAXX, IKBKG</i> | 3.61E-09 |
| Positive regulation of cellular process | 7.05E-11 | <i>JUNB, TUBB, BBC3, BOK, CDKN2A, TICAM1, MALT1, DAP, MAPK8IP2, IRAK1, CDKN1A, FOS, CCND3, IKBKG, TRIM28, MKL1, PIAS4, TRAF2, BAK1, TP53, TNFRSF1A, BCL2L1, BAX, TFE3*, BIK, TRADD, RELA*, FAS, TP73*, DAXX</i> | 9.55E-08 |
| Negative regulation of programmed cell death | 3.20E-10 | <i>TIAF1, MKL1, PEA15, TAX1BP1, MALT1, TP53, BCL2L1, HSPA1A, BAX, IRAK1, RELA*, FAS, CDKN1A, TP73*, MAPK8IP1</i> | 4.34E-07 |
| Regulation of cellular process | 7.41E-09 | <i>JUNB, TUBB, CDKN2A, MAPK12, TICAM1, MAPK8IP2, MAPK11, TOLLIP, CDKN1A, TIAF1, DIRAS1, CCNG2, PIDD, MKL1, PIAS4, TNFRSF1A, TP53, BCL2L1, BAX, RELA, TRADD, NKIRAS1, MNT, RASSF1, BBC3, MADD, BOK, TAX1BP1, TANK, PEA15, NPC2, MALT1, DAP, NKIRAS2, HSPA1A, IRAK1, GPS1, HSF1, CCND3, FOS, IKBKG, TRIM28, RASL10B, PES1, TRAF2, BAK1, TFE3*, BIK, FAS, TP73*, DAXX, MAPK8IP1</i> | 1.00E-05 |

Main GO biological processes enrichment terms for the RB DEGs 48 h after DAC treatment. *, markers of interest. RB, retinoblastoma; DEG, differentially expressed.

results have emphasized the role of ‘methylomes’ (i.e., genome-scale methylation maps obtained through high-throughput methods) in establishing cancer hallmarks (8). Among the several types of known epigenetic modifications, DNA methylation is of particular clinical interest due to its association with cancer initiation and progression, and its role as predictive biomarker for response to chemotherapy (9). Linking epigenetic changes with drug resistance may form a basis for the design of future treatments strategies combining epigenetic and chemotherapeutic regimens.

We provide comparative evidence derived from the analyses of RB and HOS cells treated with a demethylating agent (DAC). In particular, the objective of the study is to analyze the marker role of genes that were detected as differentially expressed (DEG) in both cell types, and assess the network signatures induced by these common genes by targeting both co-expression associative dynamics and interactions between their products. In earlier work (10,11), we focused on the osteosarcoma-derived HosDXR150 cell line and found that its proliferation was effectively reduced by treatment with the DAC 5-Aza-dC (decitabine) alone, among other types of inhibitors. We also obtained a DEG profile from time course microarray experiments on the

RB-derived WERI-RB1 cell line treated with 5-Aza-dC only. The DEG lists and their annotations are provided in *Tables 1,2*, considering both cancer profiles measured 48 h after DAC treatment. A Venn diagram is shown in *Figure 1* for comparative evaluations restricted to common DEGs, either up- or down-regulated.

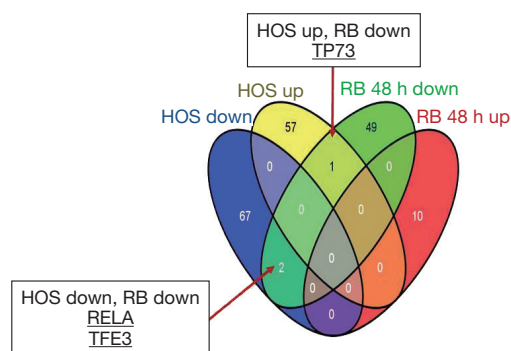
Methods

We briefly summarize the data generation aspects relevant to the novel developments, and refer the readers for further details on HOS and RB treatments to our previous work (10,11). Here, we embrace networks for inference purposes, and following known techniques (12-14).

HosDXR150 cells were treated with 2.5 μ M 5-Aza-2'-deoxycytidine (5-Aza-dC) for an incubation period of 24-96 h, in absence (control) or presence of drugs. Total RNA was isolated from treated and untreated cells after 48 h using TRIZOL reagent (Invitrogen). Subsequent cDNA microarray expression analysis was performed by using MWG Hybridization Service (MWG Biotech AG). For each experimental point 10 μ g of total RNA from the control (reference pool) and the sample (test pool) were

Table 2 Retinoblastoma (RB) pathway annotation terms (sources: KEGG, REACTOME and WikiPathways)

| Term | N. genes | P value | FDR | Associated genes |
|------------------------------------|----------|----------|----------|---|
| Apoptosis modulation and Signaling | 17 | 7.72E-25 | 1.08E-23 | <i>BAK1, BAX, BBC3, BCL2L1, BIK, BOK, CDKN2A, DAXX, FAS, FOS, IRAK1, MADD, MAP3K14, PIDD, TNFRSF1A, TOLLIP, TRADD</i> |
| Apoptosis | 14 | 5.93E-19 | 4.15E-18 | <i>BAK1, BAX, BBC3, BCL2L1, BOK, CDKN2A, FAS, IKBKG, RELA, TNFRSF1A, TP53, TP73, TRADD, TRAF2</i> |
| NF- κ B signaling | 12 | 4.93E-15 | 2.30E-14 | <i>BCL2L1, IKBKG, IRAK1, MALT1, MAP3K14, PIAS4, PIDD, RELA, TICAM1, TNFRSF1A, TRADD, TRAF2</i> |
| p53 signaling | 10 | 3.75E-13 | 1.05E-12 | <i>BAX, BBC3, CCND3, CCNG2, CDKN1A, CDKN2A, FAS, PIDD, TP53, TP73</i> |
| TNF signaling | 11 | 1.76E-12 | 4.10E-12 | <i>FAS, FOS, IKBKG, JUNB, MAP3K14, MAPK11, MAPK12, RELA, TNFRSF1A, TRADD, TRAF2</i> |
| TNF- α signaling | 9 | 1.84E-10 | 3.21E-10 | <i>BAX, BCL2L1, IKBKG, MADD, MAP3K14, TANK, TNFRSF1A, TRADD, TRAF2</i> |
| RIG-I-like receptor signaling | 8 | 8.36E-10 | 1.30E-09 | <i>IKBKG, MAPK11, MAPK12, OTUD5, RELA, TANK, TRADD, TRAF2</i> |

**Figure 1** Venn diagram of the DEG space from the DAC-treated RB- and HOS-derived cells. Measurements 48 h after DAC treatment. DEG, differentially expressed; DAC, demethylation agent; RB, retinoblastoma; HOS, human osteosarcoma.

labeled with Cy3 and Cy5 respectively. Each channel was scanned three times with increasing photomultiplier gain settings using Scanner 418/428 equipment (Affimatrix) at 10 μ m resolution, thereby ensuring coverage of the full dynamic range. The ImaGene intensity values were processed using the MAVI software package (MWG Biotech AG).

DEGs were selected by fixing 1.5-fold change (up-regulated if ≥ 1.5 and down-regulated if ≤ -1.5) in \log_2 expression ratios, statistically significant at a cutoff P value of 0.01 (Wilcoxon test). Benjamini-Hochberg correction for multiple testing was applied. For GO term analysis, biological process annotations were obtained from the

package GO database (v.2.9.0), whereas for pathway enrichment analysis the ClueGO software package (2.0.6) was used (<http://apps.cytoscape.org/apps/cluego>) (15). The statistical test used for enrichment was the right-sided hypergeometric test, and only terms with P values < 0.05 and at least three genes per term were selected, followed by a multiple testing correction using the Benjamini-Hochberg method. The pathway sources were KEGG, REACTOME and WikiPathways.

The RB-derived cell line Weri-RB1, obtained from ATCC (Rockville, MD), was treated with 5-Aza-dC (versus untreated control) in a time course experiment measuring gene expression profiles at 3 specific time points after treatment initiation, i.e., after 48, 72 and 96 h. Total RNA samples were isolated using TRIZOL (Invitrogen). After cDNA conversion, microarray expression analysis was carried out using PIQORTM Cell Death Human Sense Microarrays (Milenyi Biotech) containing 200-mer oligoprobes covering 494 human genes. Mean signal and local background intensities were obtained for each spot on the microarray images using the ImaGeneTM software package (BioDiscovery).

Assessment of gene expression profiles at the three time points was achieved by using a Cy5/Cy3 customized platform containing about 500 genes related to apoptosis, cell death and inflammation. Local background was subtracted from the signal to obtain the signal intensity, after which the Cy5/Cy3 ratio was calculated. Subsequently, the mean of the ratios of 4 spots for the same gene was computed. The ratios were normalized using the Median

Table 3 HOS pathway annotation terms (sources: KEGG, REACTOME and Wikipathways)

| Term | FDR | Associated up-regulated genes |
|--|-------------|---|
| Adipogenesis | 0.000428803 | <i>FOXO1, IGF1, IL6, IL6ST, INS, RBL2, WNT1</i> |
| positive regulation of embryonic development | 0.000535755 | <i>LHX1, NR2C2, WNT1</i> |
| Aldosterone-regulated sodium reabsorption | 0.000680062 | <i>IGF1, INS, MAPK1, SFN</i> |
| cellular iron ion homeostasis | 0.000834421 | <i>ATP6V1B1, CP, MFI2, MYC, PRMT1</i> |
| Apoptosis | 0.000835037 | <i>BNIP3L, IGF1, MYC, RELA, TNFRSF1B, TP73</i> |
| Selenium Pathway | 0.001799368 | <i>IL6, INS, RELA, XDH</i> |
| release of cytochrome c from mitochondria | 0.00181839 | <i>IL6, MYC, SFN, TP73</i> |
| dorsal spinal cord development | 0.001964131 | <i>LHX1, PBX3, WNT1</i> |
| Folate Metabolism | 0.002018507 | <i>IL6, INS, RELA, SLC19A1</i> |
| regulation of gluconeogenesis | 0.002121088 | <i>FOXO1, IL6, INS</i> |
| regulation of fat cell differentiation | 0.003519736 | <i>FOXO1, IL6, INS, WNT1</i> |
| Amyloids | 0.003981304 | <i>HIST1H4I, INS, LYZ, MFGE8</i> |
| megakaryocyte differentiation | 0.003995663 | <i>HIST1H4I, PRMT1, PSG1</i> |
| T cell activation in immune resp. | 0.007889313 | <i>IL6, MYB, TNFSF18</i> |
| endocrine pancreas development | 0.008895339 | <i>FOXO1, IL6, INS</i> |
| regulation of acute inflammatory resp. | 0.01421018 | <i>IL6, IL6ST, INS</i> |

HOS, human osteosarcoma.

and the Lowess methods. Quality filtering was applied for the calculation of the Cy5/Cy3 ratio to only spots/genes with at least in one channel a signal intensity 2-fold higher than the mean background, for then selecting up- and down-regulated genes.

GeneMania (<http://www.genemania.org/>) (16,17) was used to generate the networks, showing co-expression dynamics among the connected genes through the available Co-expression, Co-localization, Genetic interactions, Pathway, Physical interactions, Predicted and Shared protein domains (default settings). The results were imported into Cytoscape for display. GeneMania allowed an assessment of the interactions occurring at co-expression level for the DEG sets in all the measured time course profiles. The network configurations were built from the log₂ expression ratio values.

Functional enrichment was obtained with David (<http://david.abcc.ncifcrf.gov/>) and PantherDB (<http://www.pantherdb.org/>) tools for GO enrichment and pathway mapping, respectively. Pathway analysis was performed using ClueGo in Cytoscape 3.1, and by selecting as annotation sources Wikipathways, KEGG and Reactome. The statistical analysis included right-sided hypergeometric test for enrichment by Benjamini-Hochberg P value correction.

Results

GO (biological processes) and pathway annotations referred to the evidences obtained from the RB-derived cell line Weri-RB1 are listed in *Tables 1,2*, respectively. The DEG sets enrich terms according to FDR-corrected P values. Pathway annotations for the HOS-derived cell line HosDXR150 are listed in *Table 3* (up-regulated DEGs) and in *Table 4* (down-regulated DEGs), respectively. We found only 3 DEG markers that were shared between the two cancer types; one of them (*TP73*) exhibiting a discordant regulation sign (*Figure 1*). From these genes as the network seed nodes, co-expression network links (dashed lines) and protein-protein interaction networks (straight lines) were built. In the figures, the blue rectangular nodes indicate DEGs, while the grey ovals represent interactors that were added to complete the connectivity patterns.

A neighbor-1 expanded network (i.e., starting from a seed node, and including the direct links with surrounding nodes) is provided for *TP73* in both cancer types, due to the particular relevance of this gene. Only closest neighbor exploration of the seed gene was considered, to avoid redundant networks. The genes of interest are shown in *Figure 1*. Firstly, transcription factor binding to IGHM enhancer 3 (*TFE3*), which plays a role in immunity (activation of CD40L in T-cells) and is also known as a

Table 4 HOS pathway annotation terms (sources: KEGG, REACTOME and Wikipathways)

| Term | FDR | Associated down-regulated genes |
|---|-------------|---------------------------------|
| EBV LMP1 signaling | 0.001583304 | <i>IFNB1, MAPK1, RELA</i> |
| TGF- β signaling | 0.001687583 | <i>ENG, SMAD5, TFE3, WNT1</i> |
| Angiogenesis overview | 0.002127782 | <i>DAG1, MAPK1, MMP2, TIMP4</i> |
| Bladder cancer | 0.003596069 | <i>MAPK1, MMP2, MYC</i> |
| Negative regulation of epithelial cell migration | 0.003891368 | <i>ACVRL1, CXCL13, MCC</i> |
| Regulation of chondrocyte differentiation | 0.003970325 | <i>ACVRL1, RELA, SAFB</i> |
| Negative regulation of endothelial cell proliferation | 0.0061317 | <i>ACVRL1, ENG, XDH</i> |
| IL-4 signaling | 0.006646647 | <i>FES, MAPK1, RELA</i> |
| Acute & chronic myeloid leukemia | 0.008387515 | <i>MAPK1, MYC, RELA</i> |
| Regulation of cartilage development | 0.008387515 | <i>ACVRL1, RELA, SAFB</i> |

HOS, human osteosarcoma.

fusion gene associated with chromosomal translocations. Secondly, V-Rel avian reticuloendotheliosis viral oncogene homolog (*RELA*), deeply involved in *NFkB1* signaling, and related to the PI3k-Akt cascade, inflammation, immunity, differentiations, cellular growth and tumorigenic processes. Finally, *TP73* is a transcription factor participating in apoptotic response to DNA damage and essential for expressing cytokines in T-cells. It appears that the only commonly and DEG markers bring an immune system signature.

Continuing with the annotations, the *TFE3* encoded protein promotes the expression of genes downstream of TGF- β signaling. It activates the expression of *CD40L* in T-cells, thereby playing a role in T-cell-dependent antibody responses in activated CD4-positive T-cells and thymus-dependent humoral immunity. *NFkB* is a pleiotropic transcription factor ubiquitously involved in several biological processes, and encompassing *NFkB1* and *NFkB2* bound to either *RELA* or *RELB*. The activity of *NFkB* is also affected by various mechanisms of post-translational modification and sub-cellular compartmentalization, as well as by interactions with other co-factors (18).

The jointly *RELA*- and *TFE3*-induced network is denser in RB cells than in HOS ones (*Figure 2*). In particular, the *RELA* sub-networks are populated with DEGs. An interesting PIN link for *TFE3* is *TRIM28*. The latter gene encodes a protein that is localized in the nucleus, where it mediates transcriptional control by interacting with the KRAB (Kruppel-associated box) repression domain present in many transcription factors. According to the Human Gene Database annotation tool (<http://www.genecards.org/>) *TRIM28* is associated with specific chromatin regions, and

mediates epigenetic gene silencing by recruiting CHD3, a subunit of the nucleosome remodeling and deacetylation (NuRD) complex, and SETDB1 to the promoter regions of KRAB target genes. Also, it enhances transcriptional repression via increases in H3 Lys-9 methylation, and decreases in histone H3 Lys-9 and Lys-14 acetylation, and also coordinates the disposition of HP1 proteins. Finally, it acts as an inhibitor of E2F1 activity by stimulating E2F1-HDAC1 (histone de-acetylase-1) complex formation and inhibiting E2F1 acetylation. Interestingly, it participates in E2F1-mediated apoptosis in the absence of *RB1*, and mediates the transcriptional repressing activity of FOXP3 and the suppressive function of regulatory T-cells (Treg) (19). In HOS cells, the two target genes induce a much smaller network (only one co-expressed gene appears). A role in immunity is appearing but remains to be deciphered, *in view* of the evidences from the two gene markers (*RELA* and *TFE3*).

TP73 encodes a member of the *p53* family of transcription factors involved in cellular responses to stress and development. It maps to a region on chromosome 1p36 that is frequently deleted in tumors, and that is thought to contain multiple tumor suppressor genes. It participates in the apoptotic response to DNA damage, possibly as a tumor suppressor protein. Down-regulated *TP73* in RB cells (*Figure 3*) induces a small sub-network, which is expanded when neighbor-1 (indirect) interactors are linked. Among the DEGs that interact with the target, *DAXX* appears relevant. This gene encodes a multifunctional protein that interacts with a wide range of proteins, including apoptosis-related *EAS*. The indirect links with DEGS that are reached through the neighbor-1 links are, in general, functionally

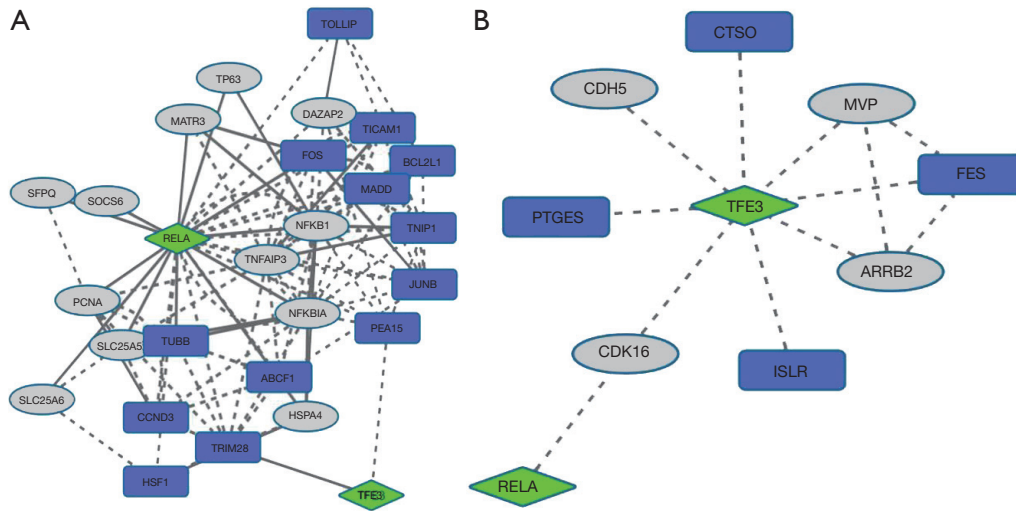


Figure 2 *TFE3* and *RELA* induced networks in RB-derived (A) and HOS-derived (B) 48 h after DAC treatment. Dotted links refer to co-expression associations, straight links refer to protein-protein interactions obtained from the Genemania tool. RB, retinoblastoma; DAC, demethylation agent.

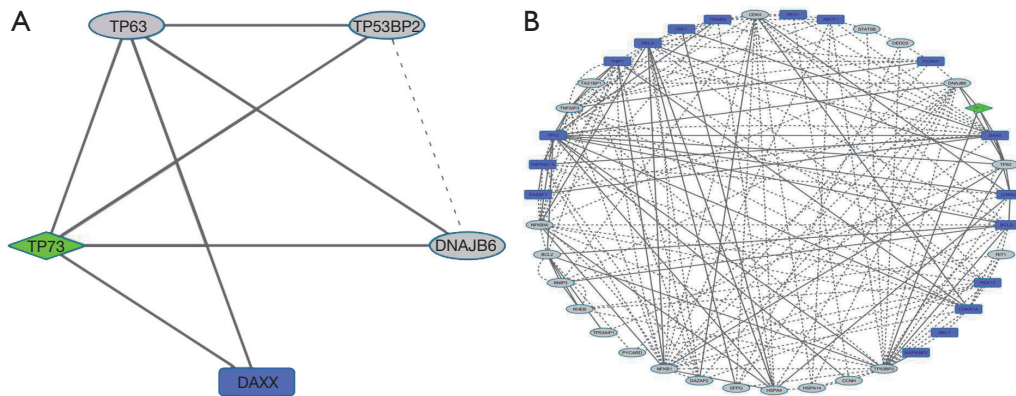


Figure 3 Directly (A) and indirectly (B) *TP73*-induced networks in RB-derived cells. RB, retinoblastoma.

relevant.

In HOS cells, *TP73* has a discordant sign (up-regulation) and the induced sub-network is entirely co-expressed. Oncogenic *WNT1* is one of the uncovered indirect associations, as also *TIMP4* which encodes an inhibitor of matrix metalloproteinases (MMPs), a group of peptidases that is involved in degradation of the extracellular matrix (Figure 4).

Conclusions

Three DEGs were identified as shared markers in two cell lines derived from associated cancers after treatment with

the same DAC. They were analyzed alone and through their induced co-expression and protein-protein interaction network dynamics. Exploiting the concept of networks and their modularity offers several advantages regarding the prediction of regulatory programs occurring at a gene ensemble scale rather than single genes.

Apart from the different sub-network configurations that are necessarily gene-specific, what is relevant from our analysis is the emergence of differential signatures for markers of two associated cancers (RB and HOS) that were both detected as DEG after DAC treatment. The evidences here presented conform with our findings from previous studies, especially indicating that ensemble network markers

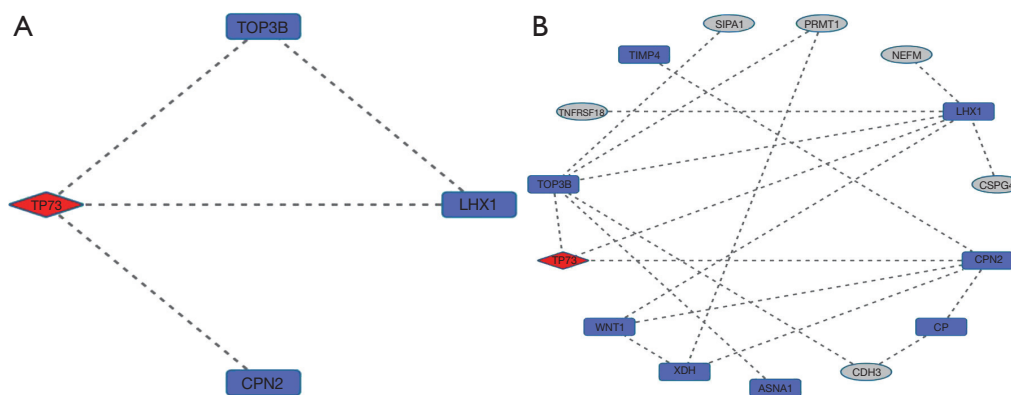


Figure 4 Directly (A) and indirectly (B) TP73-induced networks in HOS cells. HOS, human osteosarcoma.

can provide more effective disease signatures than single genes in HOS cells.

While establishing new cancer phenotypes through networks remains a valid possibility, testing is quite clearly needed on a case-by-case basis. In the present study, for instance, it was found that with three DEG markers in common between the associated cancers and considered as potentially relevant disease phenotypes, only for two of them (*RELA* and *TFE3*), and prevalently for one cancer (RB), we could find an informative network signature, according to standard annotations. Indeed, we were able to find marks of immunity-related functions and epigenetic effects.

For the *TP73* gene marker, the induced networks have shown different configurations, with the important marks of apoptosis remaining more evident in just one cancer type (RB). Both direct and indirect connectivity patterns were found to be different across the two cancers. Even after expanding the marker outreach to include more relationships across the networks compared to before, the effects did not appear to lead to homogeneous signatures. This observation was contingent in both cancers, i.e., only the closest gene and protein interactors were explored by taking advantage of the information provided by the computational tool. Further analyses could be employed with different outcomes.

The main conclusion from the examples here provided is that, despite evidence on disease phenotypes from three shared markers arising from similar experiments centered on epigenetic (DAC-driven) treatment of two associated cancers (RB and HOS), a more complete interpretation of cancer associations and/or specific versus differential role of the immune system remains hard to achieve once contextual

analyses are carried out for such markers over their induced networks signatures.

Apart from deciphering the epigenetic influences exerted on the DEG cancer patterns, one limitation of this study is that the expression profiles were obtained from microarray experiments, which are known to be of minor depth and accuracy compared to comprehensive high-throughput settings, such as RNA-Seq. Another limitation is that other types of regulation may underlie the DAC-driven phenotypes induced in the two examined cell lines, but for these possible causal influences data are not available at this time.

In order to overcome such limitations, a current direction of work is to move from cell lines to patient samples, especially with HOS, and run RNA-Seq experiments to generate data. Finally, the two tumors offer relatively limited coverage, compared to other cancers, thus need additional in-depth analyses, we are confidently looking into the direction of research named ‘integrative omics’ to provide further applications and novel insights in different primary cancers and treatment scenarios.

In conclusion, network medicine can elucidate cancer aspects by performing integrative multiscale inference on identified oncoepigenetic network signatures potentially linked to disease hallmarks. However, it emerges from the performed comparative analysis that DEG genes after epigenetic treatment build only isolated hotspots rather than cancer signatures, and therefore it would be wiser to explore differential cancer molecular profiles as those uncovered by network modules.

Acknowledgements

The author thanks C Cinti for discussions on the two

cancers and for generating the data that were published in the reported earlier work.

Footnote

Conflicts of Interest: The author has no conflicts of interest to declare.

References

1. Lee WH, Bookstein R, Lee EY. Studies on the human retinoblastoma susceptibility gene. *J Cell Biochem* 1988;38:213-27.
2. Issing WJ, Wustrow TP, Oeckler R, et al. An association of the RB gene with osteosarcoma: molecular genetic evaluation of a case of hereditary retinoblastoma. *Eur Arch Otorhinolaryngol* 1993;250:277-80.
3. Khosravi A, Shahrabi S, Shahjahani M, et al. The bone marrow metastasis niche in retinoblastoma. *Cell Oncol (Dordr)* 2015;38:253-63.
4. Hansen MF, Koufos A, Gallie BL, et al. Osteosarcoma and retinoblastoma: a shared chromosomal mechanism revealing recessive predisposition. *Proc Natl Acad Sci U S A* 1985;82:6216-20.
5. Chauveinc L, Mosseri V, Quintana E, et al. Osteosarcoma following retinoblastoma: age at onset and latency period. *Ophthalmic Genet* 2001;22:77-88.
6. Jones PA. Functions of DNA methylation: islands, start sites, gene bodies and beyond. *Nat Rev Genet* 2012;13:484-92.
7. Rodríguez-Paredes M, Esteller M. Cancer epigenetics reaches mainstream oncology. *Nat Med* 2011;17:330-9.
8. Witte T, Plass C, Gerhauser C. Pan-cancer patterns of DNA methylation. *Genome Med* 2014;6:66.
9. Baylin SB, Jones PA. A decade of exploring the cancer epigenome - biological and translational implications. *Nat Rev Cancer* 2011;11:726-34.
10. Capobianco E, Mora A, La Sala D, et al. Separate and combined effects of DNMT and HDAC inhibitors in treating human multi-drug resistant osteosarcoma HosDXR150 cell line. *PLoS One* 2014;9:e95596.
11. Malusa F, Taranta M, Zaki N, et al. Time-course gene profiling and networks in demethylated retinoblastoma cell line. *Oncotarget* 2015;6:23688-707.
12. Chen L, Liu R, Liu ZP, et al. Detecting early-warning signals for sudden deterioration of complex diseases by dynamical network biomarkers. *Sci Rep* 2012;2:342.
13. Deng S, Qi J, Stephen M, et al. Network-based identification of reliable bio-markers for cancers. *J Theor Biol* 2015;383:20-7.
14. Mora A, Taranta M, Zaki N, et al. Ensemble inference by integrative cancer networks. *Front Genet* 2014;5:59.
15. Bindea G, Mlecnik B, Hackl H, et al. ClueGO: a Cytoscape plug-in to decipher functionally grouped gene ontology and pathway annotation networks. *Bioinformatics* 2009;25:1091-3.
16. Mostafavi S, Ray D, Warde-Farley D, et al. GeneMANIA: a real-time multiple association network integration algorithm for predicting gene function. *Genome Biol* 2008;9 Suppl 1:S4.
17. Warde-Farley D, Donaldson SL, Comes O, et al. The GeneMANIA prediction server: biological network integration for gene prioritization and predicting gene function. *Nucleic Acids Res* 2010;38:W214-20.
18. Vazquez-Santillan K, Melendez-Zajgla J, Jimenez-Hernandez L, et al. NF- κ B signaling in cancer stem cells: a promising therapeutic target? *Cell Oncol (Dordr)* 2015;38:327-39.
19. Ohkura N, Kitagawa Y, Sakaguchi S. Development and maintenance of regulatory T cells. *Immunity* 2013;38:414-23.

Cite this article as: Capobianco E. Immuno-regulated common markers but different network signatures in two associated cancers: evidences from epigenetic treatment. *Ann Transl Med* 2016;4(5):86. doi: 10.21037/atm.2016.02.14